Organic &
Biomolecular
Chemistry

Cite this: *Org. Biomol. Chem.*, 2011, **9**, 4127

www.rsc.org/obc

**PAPER**

# Binding of alkaloids into the S1 specificity pocket of α-chymotrypsin: Evidence from induced circular dichroism spectra

**Ferenc Zsila,*[a] Judit Kámán,[b] Borbála Bogányi[b] and Dávid Józsvai[a]**

***Received 20th December 2010, Accepted 8th March 2011***
**DOI: 10.1039/c0ob01221a**

Non-covalent binding of planar aromatic molecules into the S1 specificity pocket of the serine protease α-chymotrypsin (αCHT) can be detected by measuring induced circular dichroism (CD) spectroscopic signals. Utilizing this phenomenon, αCHT association of proflavine (PRF), the well known serine protease inhibitor has been investigated together with plant-derived compounds including isoquinoline, pyridocarbazole and indoloquinoline alkaloids, of which αCHT binding has never been reported. Non-degenerate exciton coupling between π–π* transitions of the ligand molecules and two tryptophan residues (Trp172 and Trp215) near to the binding site is proposed to be responsible for the induced CD activity. The association constants calculated from CD titration data indicated strong αCHT association of sanguninarine, ellipticine, desmethyl-isocryptolepine and isoneocryptolepine ($K_a \approx 10^5$ $M^{-1}$) while berberine, coptisine and chelerythrine bind to the enzyme with lower, PRF-like affinity ($K_a \approx 10^4$ $M^{-1}$). PRF-trypsin and ellipticine-trypsin binding interactions have also been demonstrated. The binding of the alkaloids into the S1 pocket of αCHT has been confirmed by CD competition experiments. Molecular docking calculations showed the inclusion of PRF as well as the alkaloid molecules in the S1 cavity where they are stabilized by hydrophobic and H-bonding interactions. These novel nonpeptidic scaffolds can be used for developing selective inhibitors of serine proteases having chymotrypsin-like folds. Furthemore, the results provide a novel, CD spectroscopic based approach for probing the ligand binding of αCHT and related proteases.

## Introduction

Serine proteases are widely distributed in nature and found in all kingdoms of cellular life including viral genomes and share many biochemical and structural properties including the conserved catalytic triad (Ser, His, and Asp) that represents the main criterion for classification of a protein as a serine protease. They have diverse biochemical functions, play roles in digestion, the immune response, complement activation, cellular differentiation and hemostasis.[1–3] Structurally and catalytically similar serine proteases are grouped into 13 clans and 40 families, within which clan PA peptidases bearing the chymotrypsin-fold are the largest and best studied family.[4,5] Prototypic members of this clan are trypsin (TRP) and chymotrypsin (CHT), which cleave polypeptide chains on the C-terminal side. The secondary structure of TRP and CHT is characterized by predominance of β-sheets organized into two barrels packed with hydrophobic residues. αCHT is composed of 245 residues ($M_w$ of 25 kDa) contained in three separate polypeptide chains linked by five disulfide bridges.[6,7] The catalytic site of CHT can be divided into four distinct regions: the *n*-site where the nucleophilic attack occurs; close to the active serine is a deeply invaginated apolar pocket, the *ar*-site which binds aromatic side chains; the *am*-site (amide) which is capable of H-bonding to the substrate; and the *h*-site which accomodates the α-hydrogen of substrates.[8] The *ar*-site, known as the S1 specificity pocket (residues 185–195, 213–223 and 226–228), is the most important binding locus which controls directly the specificity and efficiency of the enzyme.[9] The active serine from the catalytic triad (Ser195) is located at the mouth of the S1 cavity. Small structural differences in the S1 pocket result in very different substrate specificity for TRP and αCHT in spite of their very similar tertiary structures and catalytic mechanism.[10] The deeply invaginated hydrophobic S1 pocket of αCHT shows high specificity for aromatic (Phe, Trp, Tyr) and bulky apolar side-chains (*e.g.* Met)[9] while in TRP, where the Ser189 residue at the bottom of the pocket is replaced by an Asp side-chain, it accommodates Lys and Arg residues.

It has been long known that certain aromatic compounds can combine with the S1 pocket of αCHT and thus can function as competitive inhibitors.[8,11,12] Among the acridine dyes, αCHT binding of proflavine (PRF) has been well documented and several reports have conclusively shown that a monomeric PRF molecule is accommodated in the S1 cavity of αCHT[13–16] and related serine proteases such as TRP[15,16] and thrombin (THR).[17] Upon binding to these enzymes, bathochromic shift of the main

[a]*Department of Molecular Pharmacology, Institute of Biomolecular Chemistry, H-1025, Budapest, Pusztaszeri u. 59-67., Hungary. E-mail: zsferi@chemres.hu; Fax: (+36) 1-438-1145*
[b]*BioBlocks Magyarország Kft., H-1045, Budapest, Berlini u. 47-49. III/105., Hungary*

VIS absorption peak of PRF can be observed. This has been exploited for calculating the affinity constant and to specifically monitor the binding of other inhibitors into the S1 pocket.[14,15,18–21] Chiral perturbation of electronic transitions of achiral molecules combined with asymmetric protein binding sites can induce positive and/or negative Cotton effects (CEs) in their circular dichroism (CD) spectrum which cannot be measured in protein-unbound state.[22–24] Analysis of such induced (or extrinsic) CD bands may add further information on the binding process. Beyond the absorption spectrophotometric studies, however, no CD spectroscopic investigation of the PRF-αCHT interaction has been performed to date. Thus, CD in combination with UV/VIS absorption spectroscopy have been employed to study the PRF binding of αCHT. Upon finding induced CD activity of PRF-αCHT complexes this methodology was extended to investigate the αCHT binding of several plant alkaloids structurally similar to PRF (Fig. 1). The benzylisoquinoline alkaloid sanguinarine (SNG) and chelerythrine (CHL) have been shown to have inhibitory effects on some enzymes, such as monoamine oxydase,[25] protein kinases,[26] peptidases[27] and elastase.[28] The protoberberine alkaloids, berberine (BRB) and coptisine (CPT), exhibit activities on an even wider scale of biomolecular targets,[29] many of them shared with SNG and CHL. Ellipticine (ELL) a pyridocarbazole framework compound is long known to express antineoplastic effects *via* DNA-intercalation and topoisomerase II inhibition[30] and inhibition of cytochrome P450 has also been reported.[31] The indoloquinoline alkaloid cryptolepine and its isomers have been shown to possess a wide range of biological activities including antimalarial, anti-inflammatory and anticancer effects.[32] However, the underlying molecular mechanism of the enzyme inhibitory action of these important natural substances is poorly understood.

## Materials and methods

### Materials

Proflavine hemisulfate dihydrate (Sigma), berberine HCl (Sigma), chelerythrine chloride (LC Lab), coptisine chloride (PhytoLab, Germany), palmatine chloride (Aldrich), sanguinarine chloride (Sigma), coralyne (Acros Organics) and ellipticine (Fluka) were used as supplied. α-Chymotrypsin (type II, protein content = 97%; 59 units $mg^{-1}$ protein) and trypsin (TPCK treated, ≥ 13961 BAEE units $mg^{-1}$) from bovine pancreas were purchased from Sigma. The

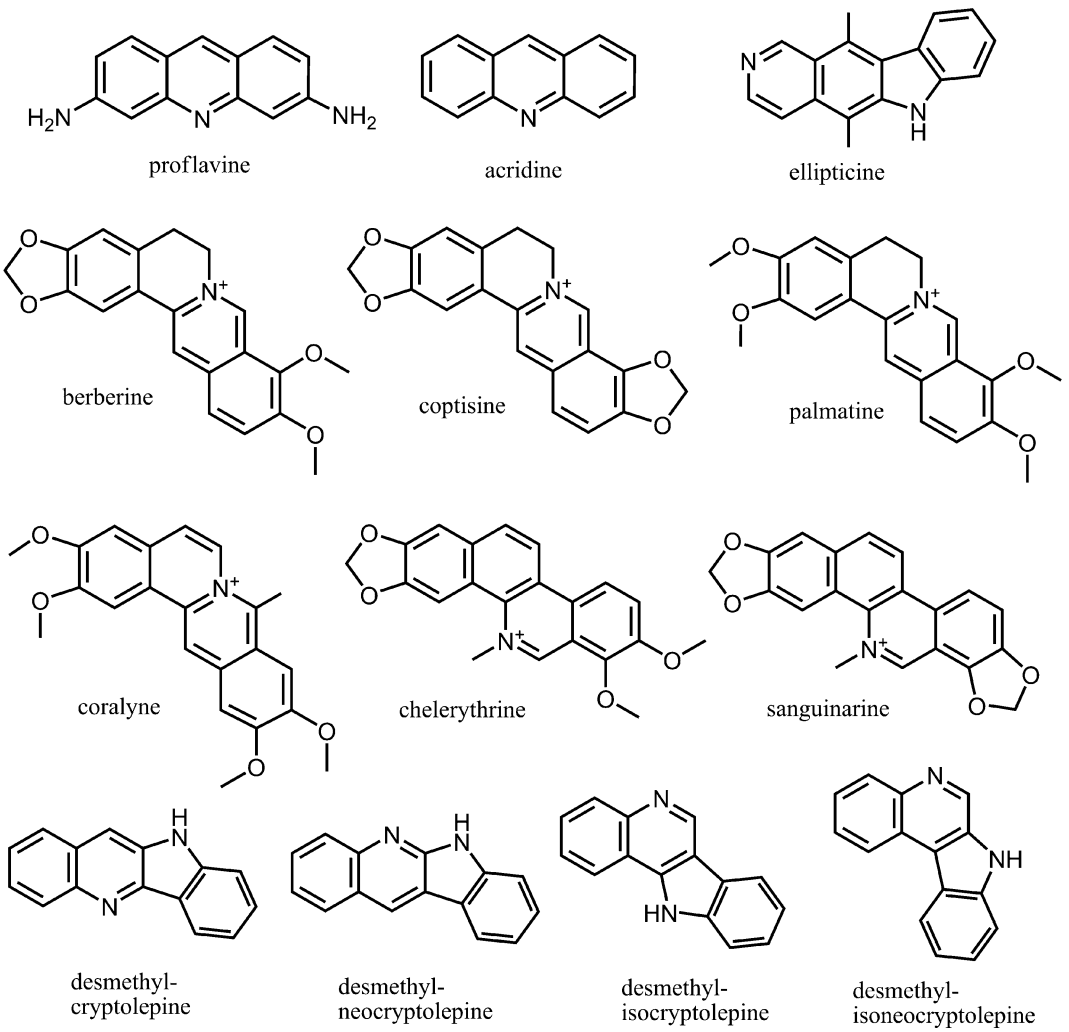


**Fig. 1** Chemical structures of proflavine, acridine and plant alkaloids studied in this work.

 

synthesis of desmethyl-cryptolepine, desmethyl-neocryptolepine, desmethyl-isocryptolepine and desmethyl-isoneocryptolepine will be published elsewhere.[33] All other chemicals were of analytical grade.

### Preparation of ligand and enzyme solutions

Ligand stock solutions (normally about $1 \times 10^{-3}$–$2 \times 10^{-3}$ M) were prepared freshly by using distilled water or ethanol. Enzyme samples were dissolved in physiological Ringer buffer solution (pH 7.4, 137 mM NaCl, 2.7 mM KCl, 0.8 mM $CaCl_2$, 1.1 mM $MgCl_2$, 1.5 mM $KH_2PO_4$, 8.1 mM $Na_2HPO_4 \cdot 12H_2O$, and 1.5 mM $NaN_3$). Molar concentrations of αCHT and TRP were determined spectrophotometrically: $\varepsilon_{282\,nm} = 51\,000\ M^{-1}cm^{-1}$ and $\varepsilon_{280\,nm} = 38\,000\ M^{-1}cm^{-1}$.

### Circular dichroism and UV/VIS absorption spectroscopy measurements

CD and UV/VIS spectra were recorded on a Jasco J-715 spectropolarimeter at 25 ± 0.2 °C. Temperature control was provided by a Peltier thermostat equipped with magnetic stirring. For recording CD spectra, rectangular quartz cells of 1 cm optical pathlength were used. Each spectrum represents the average of three scans obtained by collecting data at scan speed of 100 nm $min^{-1}$. UV/VIS absorption spectra were obtained by conversion of the high voltage (HT) values of the photomultiplier tube of the CD equipment into absorbance units. CD and absorption curves of ligand-enzyme mixtures were corrected by subtracting spectra of the enzymes. Jasco CD spectropolarimeters record CD data as ellipticity ('$\Theta$') in units of millidegrees (mdeg). The quantity of 'Θ' is converted to '$\Delta\varepsilon$' values using the equation $\Delta\varepsilon = \Theta/(32982 \times c \times l)$, where '$\Delta\varepsilon$' is the molar circular dichroic absorption coefficient expressed in $M^{-1}cm^{-1}$, '$c$' is the total molar concentration of the ligand (mol $L^{-1}$) in the sample solution, and '$l$' is the optical pathlength expressed in cm. For calculation of '$\Delta\varepsilon$' values, only the concentration of enzyme-bound ligand should be used. However, since it is unknown, CD spectra measured at low [L]/[P] ratios, when majority of the ligand molecules can be assumed to be bound, were used for the '$\Delta\varepsilon$' conversion (Table 1).

### Estimation of ligand-enzyme binding parameters from CD data

Details of the estimation of the association constants ($K_a$) and the number of binding sites ($n$) by using CD spectroscopic data have been described previously.[34] Non-linear regression analysis of the CD data measured at different [L]/[P] molar ratios was performed by the NLREG® software (statistical analysis program, version 3.4 created by Philip H. Sherrod).

### Molecular docking calculations

Docking calculations were carried out using the DockingServer.[35] A PM6 semi-empirical method (MOPAC2009) was used for energy minimization and partial charge calculation of the ligand molecules. Non-polar hydrogen atoms were merged, and rotatable bonds were defined. The X-ray structure of non-inhibited αCHT (PDB code 4CHA) was chosen because of its high quality resolution (1.7 Å) and lack of possible active site interference by covalent modification. The S1 pocket of αCHT was taken to include residues Val213-Thr219, Ser189-Asp194 and Ser217-Ser218. All water molecules, including those buried deeply in the S1 pocket, were removed from the protein coordinates prior to docking calculations. Hydrogen atoms were added to the PDB structure using AutoDockTools. The total charge of αCHT and partial charges of the atoms were calculated by the Mozyme function of MOPAC2009 software.[35] The calculated partial charges were applied for further calculations. Affinity (grid) maps of 20 × 20 × 20 Å grid points and 0.375 Å spacing were generated using the Autogrid program. AutoDock parameter set- and distance-dependent dielectric functions were used in the calculation of the van der Waals and the electrostatic terms, respectively. Docking simulations were performed using the Lamarckian genetic algorithm[36] and the Solis & Wets local search method.[37] Initial position, orientation, and torsions of the ligand molecules were set randomly. All rotatable torsions were released during docking. Each docking experiment was derived from 100 different runs that were set to terminate after a maximum of 2 500 000 energy evaluations. The population size was set to 150. During the search, a translational step of 0.2 Å, and quaternion and torsion steps of 5 were applied. The outputs of docking calculations were rendered with PyMOL (The PyMOL Molecular Graphics System, DeLano Scientific LLC, Palo Alto, CA, USA. http://www.pymol.org).

## Results and Discussion

### CD, absorption spectroscopic and computational docking investigations of PRF-αCHT interactions

Above 300 nm PRF displays a single, strong π–π* type absorption band centered around 444–445 nm in Ringer buffer solution. Upon binding to αCHT, this band is red-shifted by ≈ 5 nm (Fig. 2). Concomitantly, in the CD spectrum a positive extrinsic CE appears with a $\lambda_{max}$ value of 457 nm showing similar shape as the VIS absorption peak. Increase of the PRF concentration of the sample solution increased the intensity of the induced CD (ICD) band but the shape and position of the band remained constant. The $ICD_{max}$ values collected at increasing [PRF]/[αCHT] ratios allowed estimation of the association constant of the dye which is in a good agreement with the previously reported data (Table 1). In addition, the number of binding sites ($n$) indicates a single binding site per enzyme molecule. Structurally PRF is a rigid, completely planar compound so chiral conformational distortion of its aromatic framework as a possible origin of the observed ICD activity can be ruled out.[22] The spectroscopic profile of PRF-αCHT complexes (an extrinsic CE with similar shape and position to the allied absorption band) strongly resembles the cases when the protein-bound guest molecule is located near to aromatic, especially tryptophan residues. In such cases, coupled-oscillator (exciton) interactions between π–π* transitions of the ligand and far-UV π–π* transitions of the aromatic side chains account for the extrinsic CD activity.[24,38–40] Since the strength of CD exciton couplets depends on the product of the oscillator strength of the interacting chromophores and hence on their $\varepsilon_{max}$ values,[41] the indole ring of Trp with $\varepsilon_{max} \approx 40\,000\ M^{-1}cm^{-1}$ around 225 nm is most suited for exciton coupling. In proteins, Trp-Trp coupled oscillator interactions have been proposed to be significant even at interchromophoric distances of 10 Å.[42] The S1 pocket or slit where PRF

**Table 1** Association constants ($K_a$) of ligand-αCHT complexes and the number of binding sites per enzyme molecule ($n$) estimated from CD titration data. Molar ICD ($\Delta\varepsilon$) and absorption band extrema ($\varepsilon$) of the ligands are also shown ($\lambda_{max}$ values are in parentheses). 's' denotes shoulder

| | $\Delta\varepsilon$ ($M^{-1}cm^{-1}$) | $\varepsilon_{max} \times 10^{-3}$ ($M^{-1}cm^{-1}$) | [αCHT] (μM) | [ligand] (μM) | $K_a \times 10^{-4}$ ($M^{-1}$) | $n$ |
|---|---|---|---|---|---|---|
| PRF-αCHT | +9 (457.0) | 32 (450.6) | 28 | 6.6 | 4.1 ± 0.6 | 0.9 |
| PRF in buffer | | 40 (444.4) | | 13 | | |
| BRB-αCHT | +4 (345.8) | 22 (346.0) | 44 | 13 | 1.4 ± 0.2 | 0.9 |
| BRB in buffer | | 22 (344.6) | | 39 | | |
| CPT-αCHT | +2 (352.6) | 18 (356.4) | 38 | 9.6 | 4.1 ± 0. 6 | 0.8 |
| CPT in buffer | | 19 (356.0) | | 15 | | |
| CHL-αCHT | +9 (329.0) | 17 (339.2) | 35 | 10 | 3.1 ± 0.3 | 0.9 |
| | +7 (283.0) | 24 (317.0) | | | | |
| | –9 (262.4) | 38 (269.6) | | | | |
| CHL in buffer | | 16 (338.8) | | 33 | | |
| | | 25 (316.0) | | | | |
| | | 41 (268.0) | | | | |
| SNG-αCHT | +3 (360.2) | 24 (330.2) | 28 | 6.7 | 25 ± 2 | 0.5 |
| | –8 (328.4) | 31 (276.4) | | | | |
| | +7 (292.2) | | | | | |
| | –13 265.2) | | | | | |
| SNG in buffer | | 29 (327.2) | | 17 | | |
| | | 38 (275.0) | | | | |
| ELL-αCHT | +8 (297.0) | 36$^s$ (305.0) | 16 | 3.1 | 27 ± 4 | 0.8 |
| | | 43 (297.2) | | | | |
| ELL in buffer | | 39$^s$ (300.6) | | 4.6 | | |
| | | 42 (293.8) | | | | |
| ICR-αCHT | +5 (278.0) | 30 (273.6) | 15 | 11 | 11 ± 2 | 1.0 |
| ICR in buffer | | 27 (272.8) | | 9.1 | | |
| INC-αCHT | +6 (262.6) | 32 (258.4) | 18 | 6.6 | 14 ± 2 | 0.8 |
| | +2 (321.6) | 11 (326.4) | | | | |
| INC in buffer | | 31 (257.8) | | 9.1 | | |
| | | 11 (326.0) | | | | |
| PRF-TRP | +4 (461.6) | 40 (447.2) | 27 | 6.6 | 3.4 ± 0.6 | 0.8 |
| ELL-TRP | –2 (305.6) | 41 (302.0) | 24 | 7.4 | | |
| | | 40 (294.6) | | | | |

binds is an irregular, flattened shape whose dimensions are 10 to 12 Å by 5.5 to 6.5 Å by 3.5 to 4.0 Å.[9] Its wall contains no aromatic side-chains but there are two Trp residues in site proximity, Trp172 and Trp215 of which indol rings are situated out of the cavity.[6] According to the computational docking results, the *ca*. 11 Å long PRF molecule fits neatly into the S1 pocket and is stabilized by hydrophobic as well as intermolecular H-bonding interactions (Fig. 3). The shortest distance between PRF and Trp172/Trp215 indole rings is around 6–7 Å. Thus, this binding geometry is favorable for intermolecular exciton coupling between π–π* transitions of PRF and the Trp residues. It is of interest to note that the same pair of Trp side-chains is responsible for an exciton couplet in the far-UV CD spectrum of αCHT and chymotrypsinogen.[42] The orientation of the dye molecule docked into the S1 pocket of αCHT is highly similar to that found in the X-ray structure of the PRF-THR complex, where the Trp60 and Trp215 side-chains are also in close vicinity (6.3 and 5.5 Å) to the bound ligand[17] suggesting that PRF binding of THR might also be detected by measuring extrinsic CD signals. In both enzymes the protonated ring nitrogen of PRF forms an H-bond with the carbonyl group of Ser217 (in αCHT) or Gly219 (in THR) and one amino substituent of PRF is directed toward the solvent accessible open entrance of the S1 cavity. At the bottom of the pocket in αCHT the other amino group can make an H-bond with Thr224 and Ser189 (Fig. 3) while in THR the Ser189 is replaced by an Asp residue. Distinctly from PRF, its parent compound acridine (ACR) lacks amino groups and its ring nitrogen is unprotonated at physiological pH value. ACR-αCHT interactions produced a weak positive extrinsic CE at 255 nm, close to the highly intense UV absorption band of the dye ($\varepsilon_{max} \approx 126\,000$ $M^{-1}cm^{-1}$, spectra not shown). In concert with the moderate competitive inhibitory effect of ACR on αCHT,[11] this CE suggests the accommodation of an ACR molecule in the S1 pocket. However, no induced CD signals could be obtained with acridine orange presumably due to steric incompatibility of the bulky dimethylamino-groups (spectra not shown).

### CD, absorption spectroscopic and computational docking investigations of αCHT binding of isoquinoline alkaloids, ellipticine and indoloquinoline derivatives

Taking into consideration that PRF and other synthetic aromatic compounds bind in the S1 pocket and thus competitively inhibit the enzyme,[8,11,12] αCHT binding of some plant alkaloids with planar, extended aromatic frameworks have also been tested (Fig. 1). On the basis of the CD spectroscopic results obtained with PRF, it was anticipated that the enzyme binding of these compounds could also be verified by measuring ICD signals. Indeed, addition of BRB, CPT, CHL and SNG into a αCHT solution gave rise to extrinsic CD bands above 300 nm where intrinsic CD contribution of the enzyme is negligible (Fig. 4 and 5). It should be noted that ICD peaks associated with the UV absorption bands of the alkaloids below 300 nm could also be observed (Table 1, spectra not shown). The binding parameters estimated from CD titration data as well as the invariant spectral characteristics of the ICD curves during the titration procedures indicated the combination of alkaloids with a single protein binding site in a monomeric fashion (Table 1). While the αCHT binding affinities of BRB, CPT and CHL are close to that of PRF

 

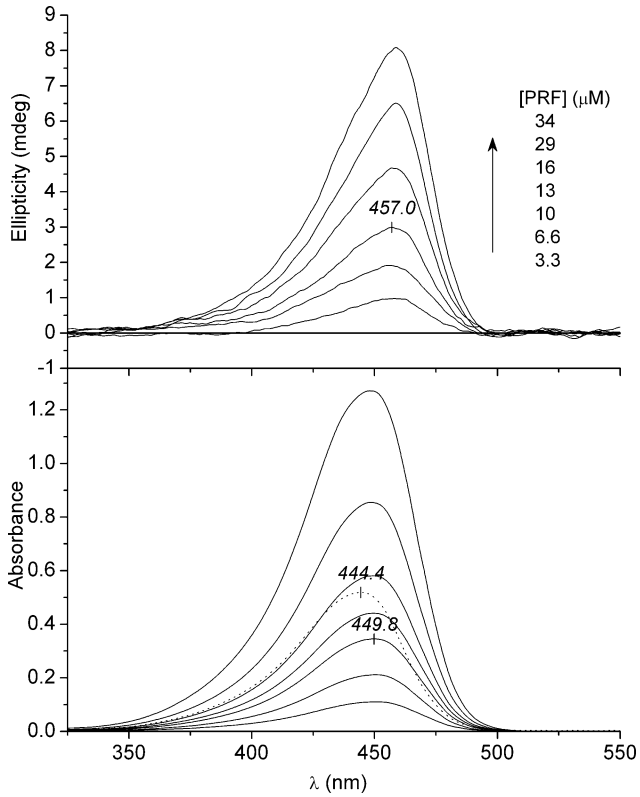


**Fig. 2** Difference CD and VIS absorption spectra obtained by titration of 28 μM αCHT with PRF (Ringer buffer, $T = 25\,^{\circ}C$). Dotted line: absorption spectrum of 13 μM PRF in protein-free Ringer buffer solution at 25 °C.

(≈$10^4$ $M^{-1}$), SNG binds to the enzyme more tightly having a $K_a$ value larger by one order of magnitude (≈$10^5$ $M^{-1}$). Comparison of the structures and binding affinities of BRB, CPT, CHL and SNG suggests that the shape and dioxolane rings of SNG result in a high degree of steric complementarity with the binding site and thus tighter binding. This is in stark contrast with the other alkaloids where bulky methoxy groups decrease the stability of the complex presumably due to steric incompatibility. This conclusion is supported by additional spectroscopic experiments performed by using palmatine and the semi-synthetic coralyne which carry methoxy substituents at both ends (Fig. 1). The difference CD spectra of these compounds measured in the presence of 46 μM αCHT showed no extrinsic CEs and their absorption curves were identical to those obtained in enzyme-free buffer solution (data not shown). The different effects of dioxolane ring-methoxy groups on the binding affinity can also be observed in the BRB-CPT relation (Fig. 1), where CPT binds to αCHT about three-times stronger than BRB (Table 1).

Taking into consideration the similarly planar framework of PRF and the isoquinoline alkaloids used here, it can be anticipated that they share a common binding site on αCHT, namely the S1 specificity pocket. To obtain experimental proof for this assumption, CD displacement measurements were carried out. ICD activity of the alkaloids belongs to their enzyme-bound forms so it should vanish upon addition of PRF if they have a common binding site. Accordingly, CEs of the alkaloids between 290–380 nm where PRF itself does not display ICD activity were monitored during the titration of CHL-αCHT and BRB-αCHT complexes with PRF. Increase of PRF concentration of the sample solutions gradually reduced the magnitude of the ICD bands of the alkaloids near to zero providing an experimental proof for their S1 cavity binding (Fig. 6).

On the basis of these data, computational docking calculations were performed to better understand the αCHT binding mode of these alkaloids. The size of the S1 pocket was found to be

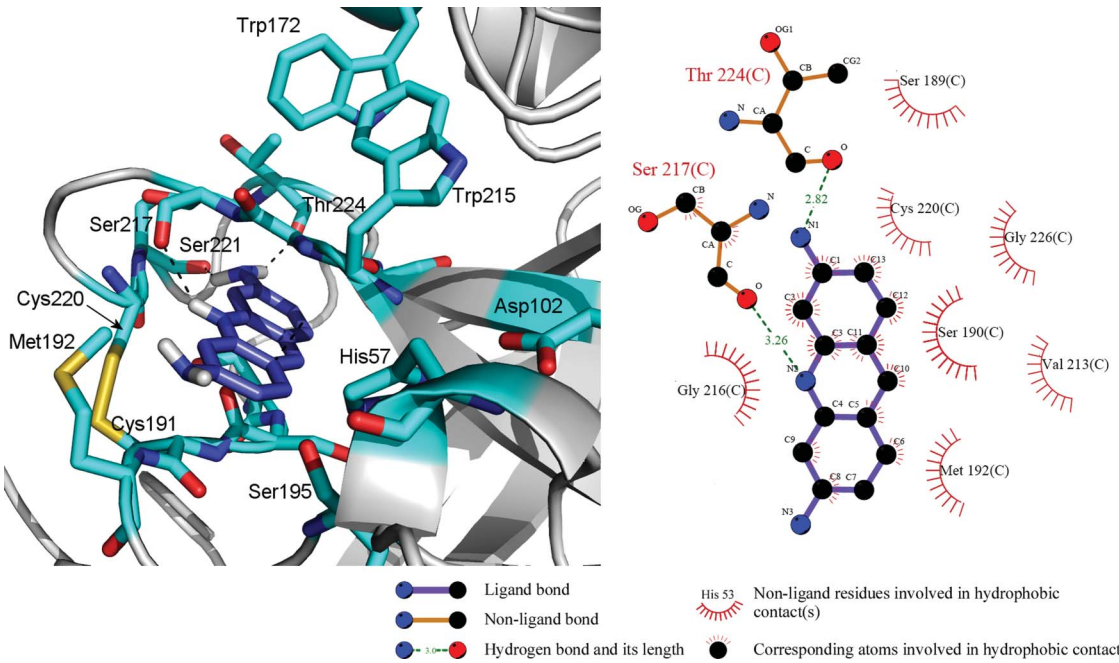


**Fig. 3** Left panel: a PRF molecule docked into the S1 cavity of αCHT viewed from the open mouth of the pocket. The catalytic triad (Ser195, His57, Asp102) and side-chains of the cavity are indicated. Right panel: a LigPlot diagram of the S1 site of αCHT with the docked PRF molecule. In both panels dashed lines represent ligand-protein residue intermolecular H-bonds.

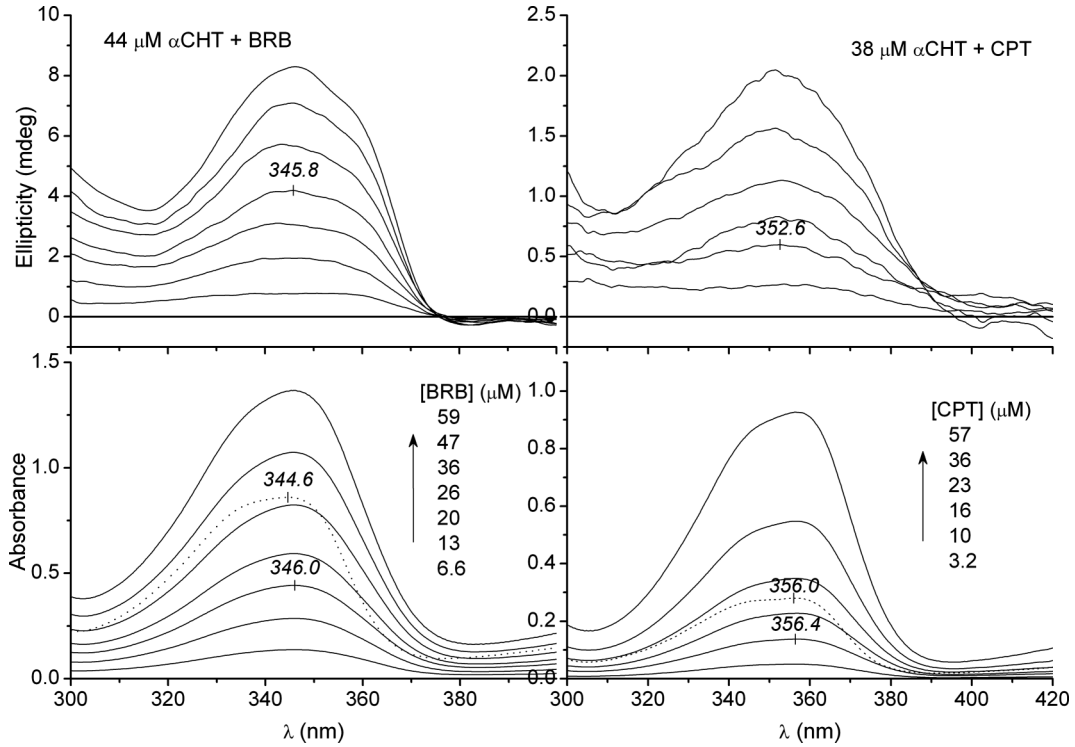


**Fig. 4** Difference CD and UV absorption spectra obtained by titration of αCHT with BRB and CPT (Ringer buffer, $T = 25\,^{\circ}C$). Dotted lines: absorption spectrum of BRB (33 μM) and CPT (15 μM) in protein-free Ringer buffer solution at 25 °C.

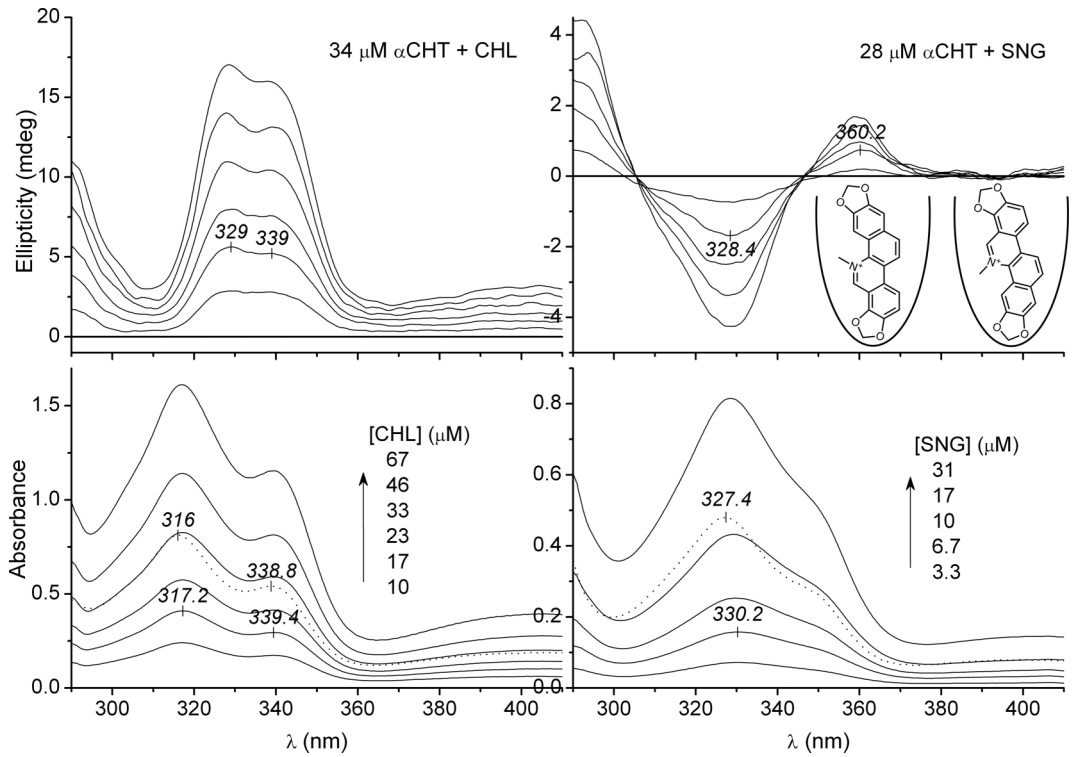


**Fig. 5** Difference CD and UV absorption spectra obtained by titration of αCHT with CHL and SNG (Ringer buffer, $T = 25\,^{\circ}C$). Dotted lines: absorption spectrum of CHL (33 μM) and SNG (17 μM) in protein-free Ringer buffer solution at 25 °C. The possibility of different binding modes of SNG in the S1 pocket of αCHT is schematically illustrated.

 

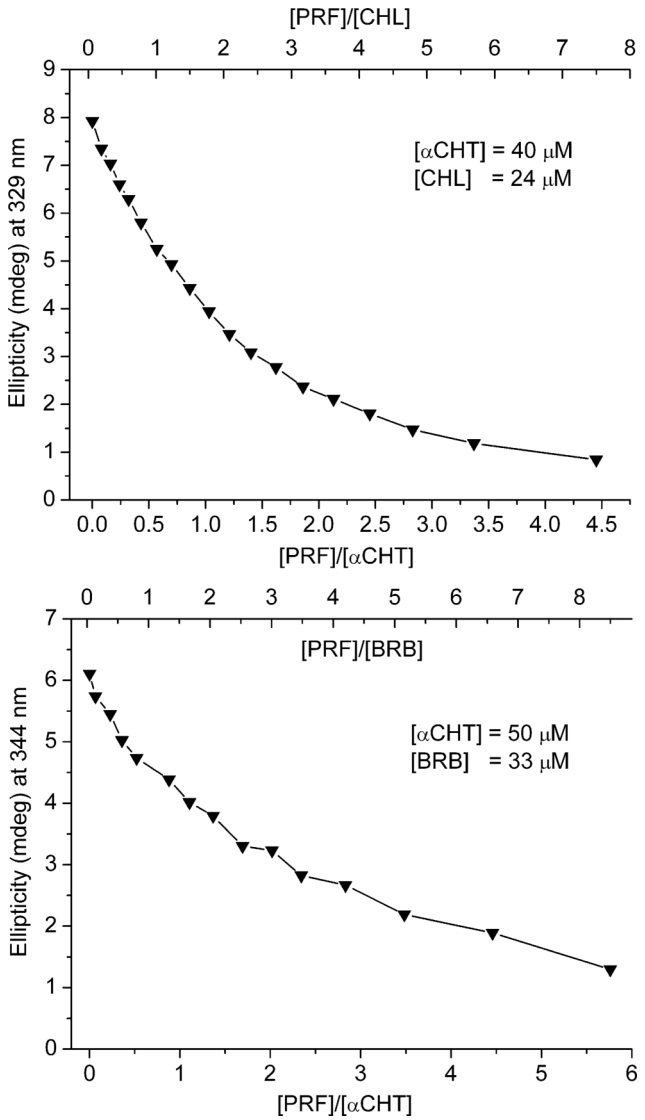


**Fig. 6** Effect of PRF on the magnitude of the positive ICD band of CHL-αCHT and BRB-αCHT complexes (Ringer buffer, $T = 25$ °C).

large enough to accommodate not only the PRF but the alkaloid molecules too, which agrees well with the results of the CD displacement experiments. Hence geometrical parameters of the S1 site render it suitable for complexing planar compounds with more extended aromatic frameworks than that of PRF. For BRB and CHL, the most frequent and best docking energy results were in which the dioxolane ring of the docked ligand points toward the bottom while the methoxy groups protrude over the entrance of the pocket (Fig. 7). This suggests that steric limitations of the binding site do not allow the reversed binding geometry where the bulky methoxy substituents would be oriented at the bottom of the cavity. The spectroscopic results obtained with palmatine and coralyne carrying methoxy groups at both ends are in full agreement with this conclusion. Within van der Waals contacts (<4 Å), the docked alkaloid molecules are surrounded by hydrophobic residues such as Val213, Gly216 and Met192 so the ligands are stabilized by hydrophobic as well as H-bonding interactions (Fig. 7). In relation to CHL and SNG, BRB penetrates deeper into the cavity: the interatomic distances between the methylene carbon atom of the dioxolane ring and the carbonyl oxygen of Ser221 at the base of the S1 site are 3.3, 4.7, and 4.8 Å for BRB, CHL, and SNG, respectively. Examination of the models reveals a steric clash between the S1 site residue Ser217 and the methyl substituent of the quaternary nitrogen of CHL and SNG which possibly impedes the deeper fit of these molecules (Fig. 7).

Notably, not only the magnitude of the association constant distinguishes SNG from the other alkaloids but also its induced CD band pattern and the anomalously low $n$ value (Table 1). In contrast to BRB, CHL and CPT which display positive CD signals between 300–400 nm, SNG exhibits both negative and positive bands (Fig. 4 and 5). The former compounds possess dioxolane moieties only at one end so their αCHT binding mode is uniform, projecting the dioxolane ring toward the bottom of the S1 cavity. Contrary to this, the structure of SNG enables alternate binding orientations (Fig. 5) which may result in opposing chirality states regarding the mutual steric disposition of the excitonically coupled chromophores of SNG and the Trp residues. Accordingly, depending on the equilibrium of these different binding modes the measured CD spectrum will be the average of two curves with chiroptical contributions different in sign and intensity.

The planar, arc-shaped pyridocarbazole ring system of ELL[30] seems to be appropriate for fitting into the S1 pocket of αCHT (Fig. 1). Addition of ELL into the solution of αCHT resulted in a positive difference CD peak around 297 nm, the position of which matches with the red-shifted absorption band of the ligand (Fig. 8). ELL displays additional UV and VIS absorption bands above 350 nm but no extrinsic CD signals could be measured in that region (not shown). In comparison to the strong UV band ($\varepsilon \approx 75\,000$ $M^{-1}cm^{-1}$) to which the ICD peak is associated, $\varepsilon$ values of ELL at longer wavelengths are much weaker (<6 000 $M^{-1}cm^{-1}$). Exciton CD band intensities are proportional to the product of the $\varepsilon$ values of the interacting identical ($\varepsilon_{max} \times \varepsilon_{max}$) or non-identical ($\varepsilon_{max}{}^{1} \times \varepsilon_{max}{}^{2}$) chromophores[41] and no appropriate signal/noise ratio can be reached with $\varepsilon$ values <10 000 $M^{-1}cm^{-1}$. Thus, low molar absorption coefficients of ELL above 350 nm do not allow measuring reliable difference CD signals. ELL possesses a protonatable pyridine nitrogen of which the p$K_a$ value has been reported to be between 6 and 7.4.[30] Hence, it is apparent that both charged (mono-cationic) and uncharged (neutral) species may coexist at physiological pH. These species can be distinguished by recording the principal UV band of ELL which undergoes dramatic changes upon protonation of the molecule.[43] Both in organic and aqueous buffer solutions the UV band of the neutral form exhibits characteristic vibronic fine structure and its $\lambda_{max}$ value is around 285–286 nm (Fig. 8). In 0.1 M HCl this band is shifted to 301 nm and shows no vibronic pattern. The loss of vibronic fine structure is inherent upon protonation and is not affected by the aqueous environment since it also occurs in organic solutions (EtOH, dioxane) upon addition of μL volume of 1 M HCl (spectra not shown). The UV spectrum of ELL measured in Ringer buffer at pH 7.4 displays an intermediate profile due to the simultaneous contribution of the charged and uncharged species: the vibronic fine structure can be seen and the $\lambda_{max}$ is around 294 nm (Fig. 8). In the presence of αCHT, the vibronic pattern is slightly suppressed and the UV band is red shifted to 297 nm and completely overlaps with the peak recorded in 0.1 M

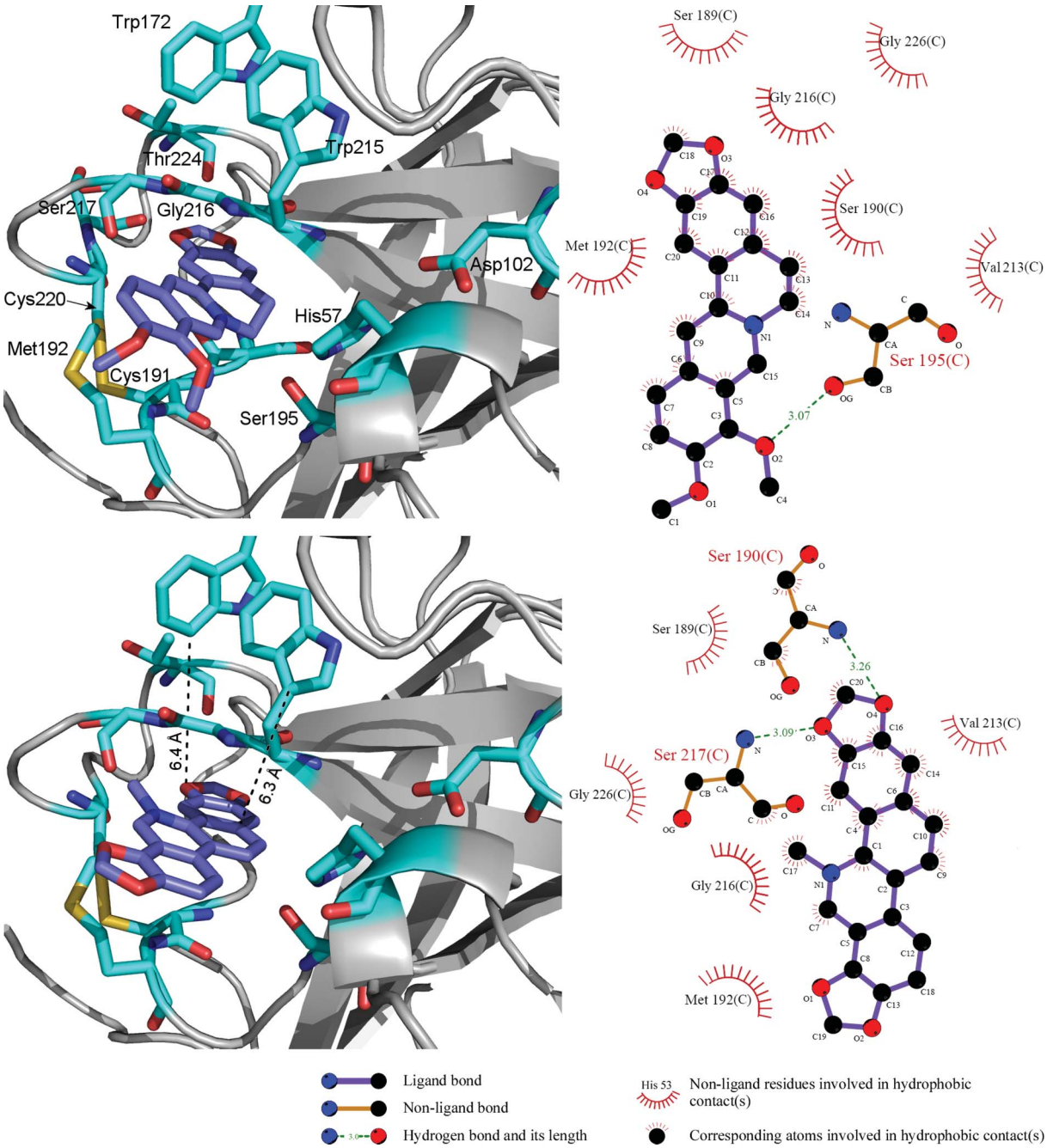


**Fig. 7** Best rank docking results of BRB (upper panel) and SNG (lower panel) to αCHT. The catalytic triad and amino acid residues of the S1 pocket are indicated with sticks. Dotted lines show intermolecular distances between SNG and Trp side-chains. 2D LigPlot representations of the ligand-enzyme interactions are shown on the right.

HCl (Fig. 8). If ELL bound to the enzyme in neutral form ($\lambda_{max}$ at 285 nm), then its $\lambda_{max}$ value should be shifted below 294 nm. It is unrealistic to assume that protein binding of this sterically rigid chromophore could result in so large a red shift which would compensate the excitation energy difference between 285 and 294 nm ($\Delta\nu = 1074\ cm^{-1}$) and that it would even shift the $\lambda_{max}$ above 294 nm. Thus, the UV spectroscopic changes observed upon αCHT binding suggest that the binding site favors the cationic species of ELL. The retention of some vibronic fine structure of bound ELL molecules can be ascribed to the effect of the well-defined protein binding environment. In order to asses the binding location of ELL, a CD displacement measurement was performed by following the changes of the ICD band of PRF-αCHT complexes (18 μM : 26 μM) upon addition of the alkaloid into the sample solution. In parallel with the increasing concentration of ELL, the magnitude of the extrinsic CE of PRF decreased and showed 50% intensity loss at 1.5 [ELL] : [αCHT] ratio (data not shown). The complete extinction of the ICD band could not be achieved due to turbidity of the sample caused by the aqueous aggregation of ELL molecules above 40 μM concentration.

 

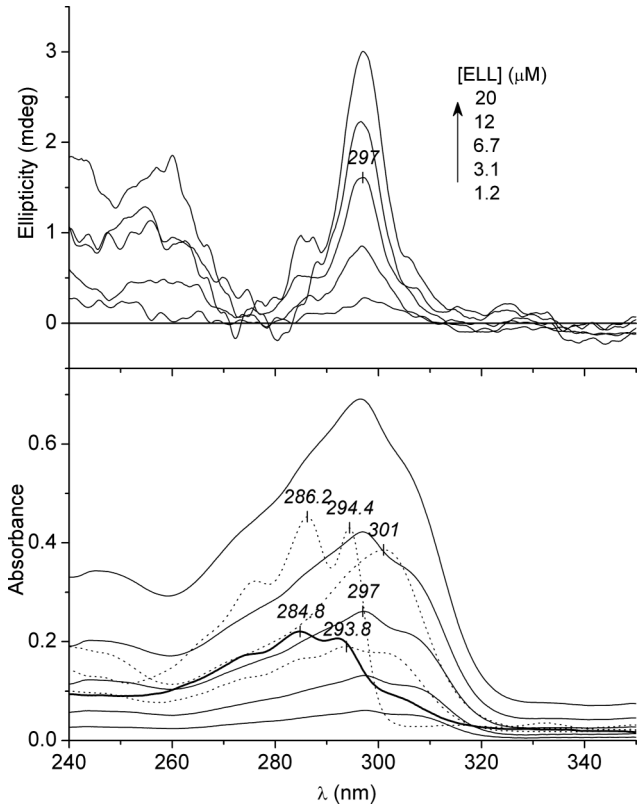


**Fig. 8** Difference CD and UV absorption spectra obtained by titration of 16 μM αCHT with ELL (Ringer buffer, $T$ = 25 °C). Dotted lines: absorption spectra of ELL in protein-free Ringer buffer (5 μM, $\lambda_{max}$ at 293.8 nm), in EtOH (8 μM, $\lambda_{max}$ at 286.2 nm) and in 0.1 M HCl (8 μM, $\lambda_{max}$ at 301.0 nm). Bold line: absorption spectrum of 5 μM ELL in 0.1 M Tris-HCl buffer at pH 8.4 ($\lambda_{max}$ at 284.8 nm).

Taking into consideration the UV spectroscopic results discussed above, the protonated form of ELL was docked into the S1 cavity of αCHT. In the most frequent best energy docking hit, the protonated pyrimidine ring is oriented toward the bottom of the pocket and forms an H-bond with the phenolic –OH group of Tyr228. In analogy with the docked PRF molecule, an additional H-bond is established between the carbazol –NH– and the carbonyl oxygen of Ser217 (Fig. 9).

αCHT binding of the desmethyl precursors of isocryptolepine (ICR) and isoneocryptolepine (INC) (Fig. 1) was also verified by measuring induced, positive amplitude difference CD bands in the same region where the UV absorption peaks of the compounds are displayed (Fig. 10). Neither the shape, sign nor energy of the induced CEs showed variation upon the increase of ligand concentration in the sample solutions. Analysis of the ICD data gave rise to the binding affinity constants which are close to that of SNG (Table 1). Comparison of the structure and CD spectroscopic profiles of these compounds to isoquinoline alkaloids and ELL refers to their analogous αCHT binding mode, *i.e.* inside the S1 pocket. Interestingly, desmethyl-cryptolepine showed only a very weak, negative-positive induced CD band pair between 260–300 nm and the use of desmethyl-neocryptolepine (Fig. 1) resulted in no difference CD signals suggesting that the positions of the indole and quinoline nitrogen atoms might be a determining factor in the αCHT binding of these compounds (data not shown). Both in the docked ICR-αCHT and INC-αCHT complex, the carbonyl oxygen of Ser217 is within H-bonding distance to the –NH– group of the alkaloid molecules which could be an additional stabilization factor beyond the hydrophobic contacts (models not shown).

### Comparison of ligand binding properties of TRP and αCHT

Binding of PRF into the S1 pocket of TRP also induces a positive CD band at 462 nm which is very similar both in shape and spectral position to the extrinsic CE of PRF-αCHT complexes (Table 1). However, molar CD intensity of the CE measured with TRP is considerably smaller which might be ascribed to the decrease of Trp residues near to the S1 site. In TRP, Trp172 is replaced by a Tyr residue of which electronic dipole allowed π–π* transition below 200 nm is separated by a larger extent in energy from the VIS transition of PRF and thus is less effective for non-degenerate coupled oscillator interaction.[44] In addition, Tyr has its $^1L_a$ band at 230 nm, with $\varepsilon_{max}$ ~10,000 $M^{-1}cm^{-1}$, much smaller than the Trp $B_b$ band at 225 nm.[42] The TRP and αCHT binding parameters of PRF estimated from CD titration data are close to each other indicating that S1 pockets of both enzymes are similarly well suited for accomodation of the dye molecule (Table 1). In sharp contrast to this situation, SNG the high-affinity ligand of αCHT showed neither CD nor absorption spectral changes in the presence of TRP (data not shown). At the base of the S1 pocket of TRP there is an Asp residue instead of Ser189 which plays an important role in the determination of substrate specificity. Most likely, the presence of the bulky Asp side-chain causes steric size restriction, so the S1 pocket of TRP is not able to accommodate large, SNG-like aromatic compounds. As found with ELL, however, planar ligand molecules comparable in size and shape with PRF can also bind in the S1 cavity of TRP. Formation of ELL-TRP complexes has been demonstrated by measuring a negative ICD band around 305 nm which is allied to the red shifted UV absorption peak of the alkaloid (Table 1). The poor ellipticity/absorbance ratio did not allow to estimate the binding parameters.

## Conclusions and future perspectives

By using CD and UV/VIS absorption spectroscopic methods this study demonstrates for the first time that the serine protease αCHT can bind isoquinoline, indoloquinoline and pyridocarbazole alkaloids featured with large, composite aromatic ring systems. Similarly to the competitive inhibitor PRF, enzyme binding of these natural agents gives rise to characteristic induced CD signals attributed to intermolecular exciton coupling between guest chromophores and the Trp172/Trp215 residues near to the binding site. The results of CD displacement experiments clearly indicated that the alkaloids and PRF share a common binding site, the S1 specificity pocket. Therefore, it is reasonable to postulate that these compounds are novel nonpeptidic competitive inhibitors of αCHT, structures of which can be utilized for developing additional specific inhibitors. The measuring of ICD signals provides a novel experimental approach for fast and simple detection of the binding of aromatic compounds into the S1 pocket of αCHT which can be extended for screening of ligand binding of additional serine proteases too. Furthermore, CD displacement

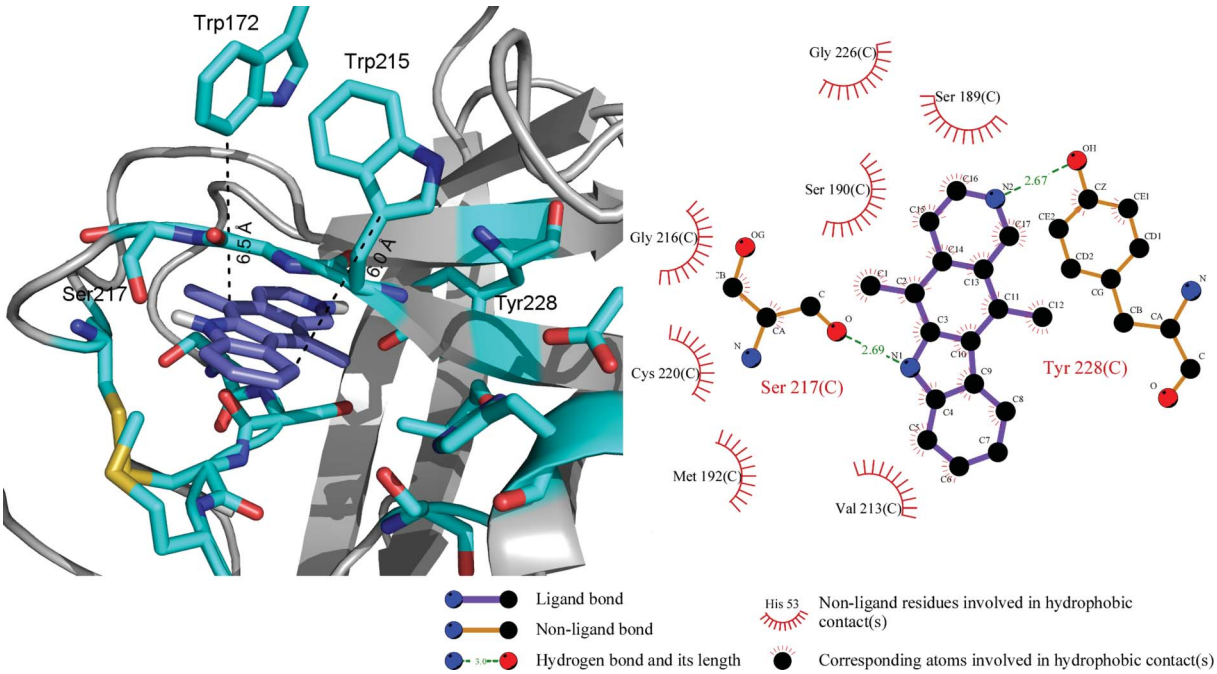


**Fig. 9** Left panel: an ELL molecule docked into the S1 cavity of αCHT viewed from the open mouth of the pocket. Only side-chains involved in H-bonding with the ligand molecule and Trp residues are labeled. Shortest intermolecular distances between ELL and Trp residues are indicated by dashed lines. Right panel: a LigPlot diagram of the S1 site of αCHT with the docked ELL molecule.

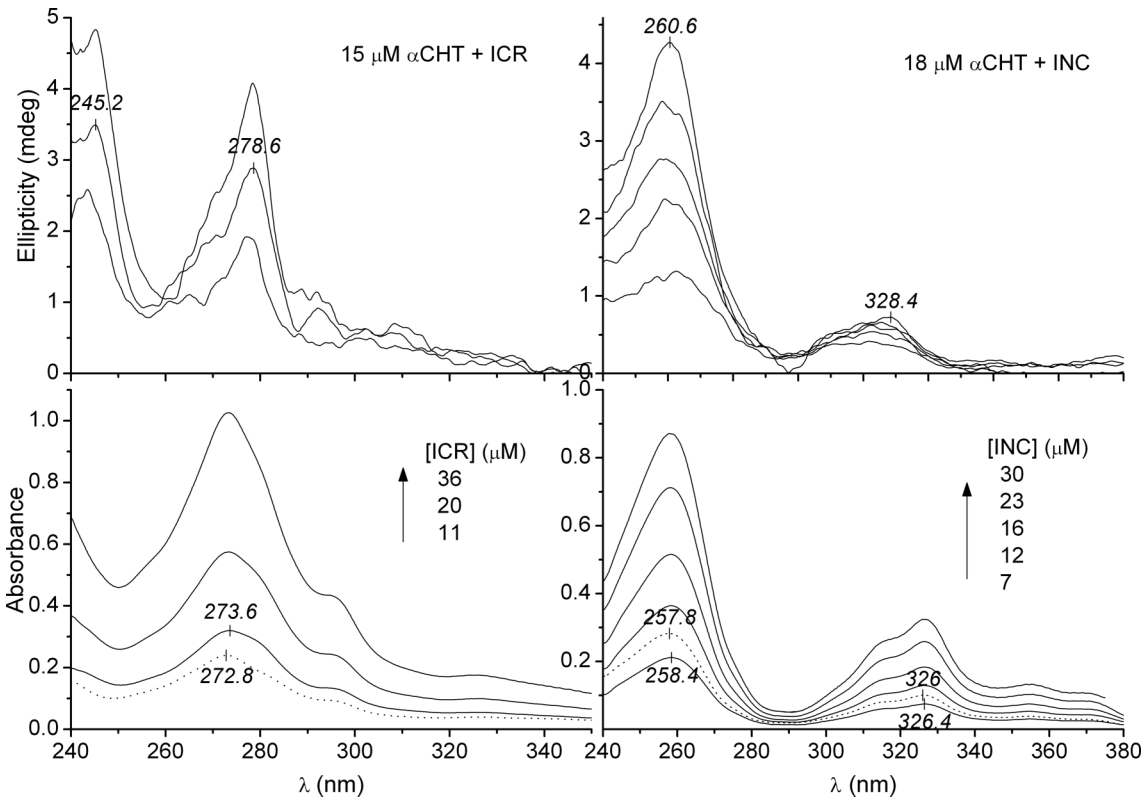


**Fig. 10** Difference CD and UV absorption spectra obtained by titration of αCHT with desmethyl-isocryptolepine (ICR) and desmethyl-isoneocryptolepine (INC) (Ringer buffer, $T = 25$ °C). Dotted lines: absorption curves of the ligands (9 μM) in protein-free Ringer buffer solution at 25 °C.

 

experiments may help to reveal competitive ligand-ligand binding interactions and to detect protease binding of optically transparent compounds (*e.g.* peptides). There is increasing evidence suggesting that serine proteases may play an important role in neural development, plasticity, neurodegeneration and neuroregeneration in the brain.[45–48] The imbalance between brain proteases and their endogenous inhibitors may lead to various pathological states.[49] In this respect, αCHT binder isoquinoline alkaloids have a potential to affect such processes since they can cross the blood-brain barrier.[50]

## Abbreviations

| | |
|---|---|
| αCHT | α-chymotrypsin |
| ACR | acridine |
| BRB | berberine |
| CD | circular dichroism |
| CE | Cotton effect |
| CHL | chelerythrine |
| CPT | coptisine |
| ELL | ellipticine |
| ICR | desmethyl-isocryptolepine |
| ICD | induced circular dichroism |
| INC | desmethyl-isoneocryptolepine |
| PRF | proflavine |
| SNG | sanguninarine |
| THR | thrombin |
| TRP | trypsin |

## Acknowledgements

This work was supported by the research grant of OTKA K69213. The generosity of some colleagues by giving commercial samples of ellipticine, palmatine, coralyne (Dr L. Biczók, Chemical Research Center, Hungary) and sanguinarine (Dr A. Bodnár, University of Debrecen, Hungary; Dr L. Kursinszki, Semmelweis University, Hungary) is highly acknowledged.

## References

1 K. M. Heutinck, I. J. ten Berge, C. E. Hack, J. Hamann and A. T. Rowshani, *Mol. Immunol.*, 2010, **47**, 1943.
2 E. Di Cera, *Mol. Aspects Med.*, 2008, **29**, 203.
3 P. Finotti, *Curr. Diabetes Rev.*, 2006, **2**, 295.
4 M. J. Page and E. Di Cera, *Cell. Mol. Life Sci.*, 2008, **65**, 1220.
5 E. Di Cera, *IUBMB Life*, 2009, **61**, 510.
6 J. J. Birktoft and D. M. Blow, *J. Mol. Biol.*, 1972, **68**, 187.
7 W. Appel, *Clin. Biochem.*, 1986, **19**, 317.
8 T. N. Pattabiraman and W. B. Lawson, *J. Biol. Chem.*, 1972, **247**, 3029.
9 T. A. Steitz, R. Henderson and D. M. Blow, *J. Mol. Biol.*, 1969, **46**, 337.
10 B. Jelinek, J. Antal, I. Venekei and L. Graf, *Protein Eng., Des. Sel.*, 2004, **17**, 127.
11 R. A. Wallace, A. N. Kurtz and C. Niemann, *Biochemistry*, 1963, **2**, 824.
12 K. D. Stewart, J. A. Bentley and M. Cory, *Tetrahedron Comput. Methodol.*, 1990, **3**, 713.
13 H. Weiner and D. E. Koshland, Jr., *J. Biol. Chem.*, 1965, **240**, 2764.
14 S. A. Bernhard, B. F. Lee and Z. H. Tashjian, *J. Mol. Biol.*, 1966, **18**, 405.
15 G. Feinstein and R. E. Feeney, *Biochemistry*, 1967, **6**, 749.
16 A. N. Glazer, *Proc. Natl. Acad. Sci. U. S. A.*, 1965, **54**, 171.
17 E. Conti, C. Rivetti, A. Wonacott and P. Brick, *FEBS Lett.*, 1998, **425**, 229.
18 E. Antonini, P. Ascenzi, M. Bolognesi, E. Menegatti and M. Guarneri, *J. Biol. Chem.*, 1983, **258**, 4676.
19 R. F. Wong, T. L. Chang and R. D. Feinman, *Biochemistry*, 1982, **21**, 6.
20 K. Inouye, B. Tonomura and K. Hiromi, *J. Biochem.*, 1979, **85**, 601.
21 A. L. Fink, *Biochemistry*, 1974, **13**, 277.
22 F. Zsila, Z. Bikádi, I. Fitos and M. Simonyi, *Curr. Drug Discovery Technol.*, 2004, **1**, 133.
23 F. Zsila, *Anal. Biochem.*, 2009, **391**, 154.
24 F. Zsila, J. Visy, G. Mády and I. Fitos, *Bioorg. Med. Chem.*, 2008, **16**, 3759.
25 S. S. Lee, M. Kai and M. K. Lee, *Phytother. Res.*, 2001, **15**, 167.
26 B. H. Wang, Z. X. Lu and G. M. Polya, *Planta Med.*, 2007, **63**, 494.
27 A. Sedo, R. Malik, J. Vicar, V. Simanek and J. Ulrichova, *Physiol. Res.*, 2003, **52**, 367.
28 T. Tanaka, K. Metori, S. Mineo, M. Hirotani, T. Furuya and S. Kobayashi, *Planta Med.*, 2007, **59**, 200.
29 E. V. Da-Cunha, I. M. Fechinei, D. N. Guedes, J. M. Barbosa-Filho and M. S. Da Silva, *Alkaloids: Chem. Biol.*, **62**, 1.
30 N. C. Garbett and D. E. Graves, *Curr. Med. Chem.: Anti-Cancer Agents*, 2004, **4**, 149.
31 C. L. Miranda, M. C. Henderson and D. R. Buhler, *Toxicol. Appl. Pharmacol.*, 1998, **148**, 237.
32 E. V. Kumar, J. R. Etukala and S. Y. Ablordeppey, *Mini-Rev. Med. Chem.*, 2008, **8**, 538.
33 B. Bogányi and J. Kámán, to be published.
34 F. Zsila, Z. Bikádi and M. Simonyi, *Biochem. Pharmacol.*, 2003, **65**, 447.
35 Z. Bikádi and E. Hazai, *J. Cheminf.*, 2009, **1**, 15.
36 G. M. Morris, D. S. Goodsell, R. S. Halliday, R. Huey, W. E. Hart, R. K. Belew and A. J. Olson, *J. Comput. Chem.*, 1998, **19**, 1639.
37 F. J. Solis and R. J. B. Wets, *Math. Oper. Res.*, 1981, **6**, 19.
38 F. Zsila and Y. Iwao, *Biochim. Biophys. Acta, Gen. Subj.*, 2007, **1770**, 797.
39 T. W. Athey and R. E. Cathou, *Immunochemistry*, 1977, **14**, 397.
40 R. A. Edwards and R. W. Woody, *J. Phys. Chem.*, 1983, **87**, 1329.
41 M. P. Heyn, *J. Phys. Chem.*, 1975, **79**, 2424.
42 I. B. Grishina and R. W. Woody, *Faraday Discuss.*, 1994, **99**, 245.
43 F. Terce, J. F. Tocanne and G. Laneelle, *Eur. J. Biochem.*, 1982, **125**, 203.
44 H. Nishino, A. Kosaka, G. A. Hembury, K. Matsushima and Y. Inoue, *J. Chem. Soc., Perkin Trans. 2*, 2002, 582.
45 Y. Wang, W. Luo and G. Reiser, *Cell. Mol. Life Sci.*, 2007, **65**, 237.
46 S. M. Chou, A. Taniguchi, H. S. Wang and B. W. Festoff, *J. Neurol. Sci.*, 1998, **160**, S73.
47 R. B. Nelson and R. Siman, *J. Biol. Chem.*, 1990, **265**, 3836.
48 S. Shiosaka, *Anat. Sci. Int.*, 2004, **79**, 137.
49 W. Luo, Y. Wang and G. Reiser, *Brain Res. Rev.*, 2007, **56**, 331.
50 X. Wang, D. Xing, W. Wang, F. Lei, H. Su and L. Du, *Neurosci. Lett.*, 2005, **379**, 132.